Journal of Autoimmunity 105 (2019) 102309

Contents lists available at ScienceDirect

Journal of Autoimmunity

journal homepage: www.elsevier.com/locate/jautimm

Phosphatidylethanolamine binding protein-4 (PEBP4) is increased in IgA nephropathy and is associated with IgA-positive B-cells in affected kidneys

Scott Taylor, Kyriaki Pieri, Paolo Nanni, Jure Tica, Jonathan Barratt, Athanasios Didangelos*

University of Leicester, Mayer IgA Nephropathy Laboratory, University Road, LE1 7RH, Leicester, United Kingdom

ARTICLE INFO

Keywords:
IgA nephropathy (IgAN)
PEBP4
Urine
Proteomics
Biomarker
B-Cells

ABSTRACT

IgA nephropathy (IgAN) is the most common glomerulonephritis worldwide and a major cause of chronic kidney disease and failure. IgAN is driven by an autoimmune reaction against galactose-deficient IgA1 that results in the generation of autoantibodies and large IgG-IgA immune complexes. Immune complexes accumulate in the glomerular mesangium causing chronic inflammation and renal scarring. A significant proportion of IgAN patients develop end-stage kidney disease and require dialysis or transplantation. Currently, there are no approved specific therapies that can ameliorate the systemic autoimmune reaction in IgAN and no biomarkers that can predict renal inflammation and scarring. In this study, we used shotgun LC-MS/MS proteomics to compare small volumes of urine from healthy subjects and IgAN patients. We identified multiple urine proteins with unknown renal or IgAN function. Our attention was captured by the increase of phosphatidylethanolamine binding protein-4 (PEBP4) in IgAN urine. The function of PEBP4 in IgAN or renal disease is unknown. Increased levels of urine and serum PEBP4 were subsequently validated in different cohorts of IgAN patients and PEBP4 was linked to declining kidney function in IgAN. Strong PEBP4 staining was sporadically seen in IgAN kidney biopsies, colocalising with IgA in glomeruli and in the lumen of kidney tubules. In a small number of IgAN biopsies, PEBP4 colocalised with IgA and CD19 while the increased excretion of PEBP4 in IgAN urine was accompanied by increased excretion of classic B-cell factors BAFF, BCMA and TACI as well as IgA and IgG. PEBP4 is a new IgAN-related protein with unknown function and a likely renal disease marker in urine and serum.

1. Introduction

IgA Nephropathy (IgAN) is a disease with autoimmune etiology and the most common primary glomerulonephritis worldwide affecting ~1-million people and a major cause of chronic nephropathy and kidney failure [1]. The disease is caused by the production of aberrantly glycosylated (galactose-deficient) immunoglobulin-A1 (IgA1) by activated B-cells present in the bone marrow [2]. Abnormal O-glycosylation of IgA, triggers the generation of autoantibodies and results in the formation of circulating immune-complexes containing galactose-deficient IgA1 plus autoreactive IgA and IgG. IgAN is associated with higher levels of serum IgA, galactose-deficient IgA1 [3,4] and IgA-IgG immune-complexes where IgA1 is the predominant subclass [5] while IgG2 has been shown to be positively correlated with elevated serum IgA in IgAN patients [6]. While the formation of anti-IgA immune-complexes is a systemic autoimmune reaction and there is no primary renal abnormality, the kidney is affected by chronic accumulation of these large, immune-complexes on the mesangium [7]. In response, mesangial cells undergo classic inflammatory and fibroproliferative activation. This cellular response is subtle and persistent and drives localised inflammation with infiltration of macrophages involved in tissue remodeling, as well as B- and T-cells targeting the IgA autoantigens [8]. Ultimately, IgA immune-complex-mediated inflammation drives glomerular and tubulointerstitial scarring with podocyte and proximal tubule cell injury [7,9]. The pathogenesis of IgAN remains obscure and our understanding of how IgA immune-complexes drive inflammation and tissue remodeling is also limited [10]. Other than generic treatment of hypertension and inhibition of the rennin-angiotensin system, there are no specific (non-experimental) therapies that can prevent either the generation of galactose-deficient IgA or the autoimmune reaction and concomitant renal inflammation and scarring caused by immune-complexes [11]. As a result, around 20% of IgAN patients develop renal failure and require dialysis or transplantation [1]. Diagnosis and risk stratification in IgAN are currently based on a kidney biopsy, which carries significant morbidity and there are no serum or urine markers with sufficient specificity to diagnose IgAN or predict which patients might progress to kidney failure [12,13].

In an attempt to identify unknown bioactive proteins and possible

* Corresponding author.
E-mail address: ad482@leicester.ac.uk (A. Didangelos).

https://doi.org/10.1016/j.jaut.2019.102309
Received 25 April 2019; Received in revised form 17 July 2019; Accepted 24 July 2019
Available online 09 August 2019

disease markers in IgAN urine, we set out to develop clinically-relevant proteomics methodology using very small volumes of patient urine and optimized simple biochemical processing. During methodology optimisation for shotgun urine proteomics, we discovered an increase in phosphatidylethanolamine binding protein-4 (PEBP4) in IgAN urine. The biological function of PEBP4, first discovered in 2004 [14], is incompletely understood and has been scarcely studied in different cancers [15]. Nothing is known about its expression and possible function in IgAN or in the kidney. The discovery and upregulation of PEBP4 in IgAN urine as well as its apparent relationship with IgA and B-cells in the kidney is described here for the first time.

2. Materials and methods

2.1. Urine processing for proteomics analysis

During proteomics methodology optimisation, we compared 2 urine pools generated from an initial cohort of 16 healthy subjects, versus 2 pools generated from the urine of 16 biopsy-confirmed IgAN patients (2 pools of 8 urines for each group). Proteomics was used to screen the urine proteome and obtain an explorative overview of differential protein levels, rather than for extensive statistical analysis. We used archived urine samples from the Leicester renal bioarchive for the initial analysis. Urine samples were spun before storing to remove cells and cellular debris. To improve the analytical depth and dynamic range of proteomics, urines were filtered and desalted (7kD cut-off spin-columns) followed by depletion of albumin and IgG using pre-packed antibody-based depletion spin-columns (Thermo, top-2 depletion kit), given that albumin and IgG are the major "contaminant" proteins in chronic kidney disease urine. Please note that for subsequent validation ELISA measurements the urine was not subject to albumin/IgG depletion. Importantly, we used just 500 µl of lyophilised desalted/albumin-depleted urine per LC-MS/MS replicate. Miniaturisation is key in clinically-relevant studies aimed at extracting maximum information with the least technical manipulation from potentially scarce or old clinical samples. For proteomics analyses, 2 µg of desalted and albumin/IgG-depleted urinary protein from each sample, were dissolved in 45 µl of 100 mM triethylammonium bicarbonate buffer, reduced with 2 mM TCEP (tris-2-carboxyethyl-phosphine) and alkylated with 15 mM chloroacetamide. Protein digestion was performed adding 5 µl of trypsin (100 ng/µl in 10 mM HCl) and enhanced by using a microwave instrument (Discover System, CEM) for 30 min at 5W and 60 °C. Samples were dried in a SpeedVac and dissolved in 20 µl of 0.1% formic acid for LC-MS/MS analysis.

2.2. Liquid-chromatography tandem mass-spectrometry (LC-MS/MS) of urine pools

3 µl (2 µg) of processed urine samples were injected on a nanoAcquity UPLC (Waters) connected to a Q-Exactive mass spectrometer (Thermo) equipped with a Digital PicoView source (New Objective). Solvent composition at the two channels was 0.1% formic acid for channel A and 0.1% formic acid, 99.9% acetonitrile for channel B. Peptides were trapped on a Symmetry (Waters) C18 trap-column (5 µm, 180 µm × 20 mm) and separated on a BEH300 (Waters) C18 column (1.7 µm, 75 µm × 150 µm) at a flow rate of 250 nl/min using a gradient from 1% to 40% acetonitrile in 90 min. The mass spectrometer was operated in data-dependent mode (DDA), acquiring full-scan MS spectra (350–1500 m/z) at a resolution of 70,000 at 200 m/z (mass to charge) after accumulation to a target value of 3,000,000, followed by HCD (high-energy collision dissociation) fragmentation on the 12 most intense signals per MS cycle. HCD spectra were acquired at a resolution of 35,000 using normalised collision energy of 25 and a maximum injection time of 120 ms. Automatic gain control (AGC) was set to 50,000 ions. Charge state screening was enabled and singly and unassigned charge states were rejected. Only precursors with intensity above 8300 were selected for MS/MS (2% underfill ratio). Precursor masses previously selected for MS/MS were excluded from further selection for 30s, and the exclusion window was set at 10 ppm. The samples were acquired using internal lock mass calibration on m/z 371.1010 and 445.1200. Acquired raw MS/MS files were converted to Mascot Generic Format (.mgf) using ProteoWizard (http://proteowizard.sourceforge.net/) and proteins were identified using the Mascot search engine (Matrix Science, version 2.5.1.3.) searching data against the Swissprot human database (version 2018-07-18). Carbamidomethylation of cysteine was set as fixed modification while methionine oxidation was set as variable. Enzyme specificity was set to trypsin allowing a maximum of two missed-cleavages. Precursor and fragment tolerance was set to 0.03Da and 10 ppm, respectively. The Mascot.dat file results were loaded in Scaffold (Proteome Software) to validate peptide and protein identifications, to visualize and count peptide and spectra identifications. The maximum false-discovery rate was set to 0.01 for peptides and 0.05 for proteins. Only proteins identified with at least 2 peptides were considered for follow up analysis. More information on proteomics analysis can be found in previous work [16]. Protein-protein interaction network analysis of genes and proteins was performed using StringDB v11 and Cytoscape (v3.6.1). BinGO was used in Cytoscape to identify Gene Ontology (GO) annotations.

2.3. Elisa

ELISA analysis was used to detect different proteins in urine as described in Results. Urine was used at 1/10 dilution (10 µl of urine and 90 µl of ELISA diluent unless otherwise stated) and ELISAs were performed using kit instructions and supplied reagents and standards in duplicate. Please note that in contrast to the urine used for proteomics, urine samples used for ELISA were not albumin/IgG-depleted. PEBP4, CTSZ, and J-Chain were detected using kits from Abbexa. BAFF kit was from Bio-Techne. BAFF-R, IFNG, TACI, BCMA and TGFB1 kits from Abcam. IgA, IgG and secretory IgA (sIgA) were measured by custom-made (in-house developed) ELISAs [17,18]. Briefly, human IgA, IgG (both DAKO) or IgA secretory component (Sigma) rabbit antibodies, were coated on Nunc MaxiSorp ELISA plates (1/1000 antibody in PBS) for 24 h followed by 2 h blocking in 5% BSA. Coated plates were then incubated with urine diluted 1/10 for IgA or 1/100 for IgG in PBS for 16 h at 4 °C, alongside NIBSC stock IgA and IgG standards (1 mg/ml) in serial dilutions using PBS. Following extensive washing in PBS with tween-20, plates were covered with HRP-conjugated anti-human IgA and IgG antibodies (DAKO) for 2 h, washed and developed using OPD and stable peroxide substrate (Thermo) for 5min. ELISA Reactions were stopped using 2 M H_2SO_4 and immediately read at 492 nm. For the custom-made secretory IgA ELISA [17], the procedure was identical to the IgA ELISA described above but the plate was first coated with rabbit antibodies (1/1000 dilution) against human secretory IgA component (Sigma) for 24 h. Secretory IgA was detected using HRP-conjugated anti-human IgA (DAKO) as above. For estimation of all different protein levels in urine by ELISA, background absorbance was subtracted from all standard and experimental sample absorbance values. No outliers were removed. All urine ELISA concentrations were corrected to urine creatinine to take into account renal filtration and urine concentration [19]. Urine creatinine was detected using a colorimetric 96-well plate kit and 5 µl of healthy or IgAN urine according to instructions (QuantichromTM; BioAssay).

2.4. Fluorescence immunohistology

For tissue staining we used archived needle kidney biopsies with a proven diagnosis of primary IgAN or biopsies reported as normal (from healthy kidney transplant donors). We also used biopsies from patients diagnosed with Lupus nephritis. Needle biopsies were fixed in 10% formalin for 48 h before automated paraffin block embedding. Dried blocks were then sectioned on a Leica microtome at 10 µm per section.

Sections were treated using acid-based antigen retrieval and de-waxing solution (Abcam) at 98 °C for 1 h. Sections were thoroughly washed, blocked in 10% normal donkey serum (Dako) for 1 h and subsequently incubated with primary antibodies: rabbit PEBP4, mouse CD64 and mouse Vimentin from Abcam, goat IgA1 (Sigma) and mouse CD19 (BioTechne) at 1/100 dilution in 10% donkey serum for 16 h at 4 °C. Sections were washed 4 times in PBS and then incubated with fluorescent secondary antibodies as described. Anti-rabbit 568 nm, anti-mouse 488 nm or 647 nm and anti-goat 488 nm. Sections were washed again 4 times and were covered in Vectashield anti-fade mounting solution. Finally staining was visualised in a Zeiss Axioscope microscope using a TissueFaxs stage and image scanning multispectral software (TissueGnostics).

2.5. Gel electrophoresis immunoblotting and sample dot-blots

Immunoblotting against PEBP4 was performed on 1 million cells per condition as described in Results. Cells were lysed in 0.2% SDS containing proteinase inhibitors (Sigma), protein concentration was estimated (A280nm) and samples were mixed with 4x Laemli sample buffer and boiled at 98 °C for 10min. 20 μg of protein per sample were loaded on 4–12% NuPAGE mini-gels (Thermo), proteins were transferred on nitrocellulose membrane, blocked in 10% milk for 1 h and incubated in rabbit PEBP4 antibodies (Abcam) diluted in 5% BSA at 1/500 dilution for 16 h at 4 °C. Goat anti-myeloperoxidase (BioTechne) was used at the same dilution. Membranes were washed 4 times in PBS-tween and incubated with HRP-conjugated swine anti-rabbit or rabbit anti-goat antibodies (Dako; 1/2000) for 1 h at room temperature. Membranes were washed again 4 times in PBS-tween and exposed to ECL-prime developing reagent (Amersham). Finally, signals were visualised in a Bio-Rad imaging system. Mouse beta-actin (Abcam) served as the loading control, detected with HRP-conjugated rabbit anti-mouse antibodies. Dot-blots were performed on nitrocellulose membranes. 1 μl of urine was used per dot. Membranes were air-dried for 1 h, blocked (10% milk in PBS), incubated with PEBP4 and secondary HRP antibodies and developed as described above.

2.6. Human samples and specimens

Ethical approval for this study and for collection of biofluids was obtained from the Northamptonshire, Leicestershire, and Rutland Ethics Committee (UHL 09873). We compared different cohorts of healthy and patient urine and serum samples as indicated in Results. First, we used 25 archived IgAN urines (patients with diagnosed, biopsy-proven IgAN) and 25 age and sex matched urine samples from subjects without renal pathology, used as healthy controls, for urine ELISAs as indicated. For comparison, we also used 14 archived urine samples from patients with diagnosed non-IgAN renal disease as indicated in Results. All healthy, IgAN and renal disease samples were collected during scheduled clinical monitoring at the John Walls Renal Unit, University Hospitals of Leicester NHS Trust. Second, we also used 25 biopsy-proven IgAN patients with low estimated glomerular filtration rate (eGFR) (25–53 ml/min/1.73 m^2; group IgAN-1; mean age 43.2) and 25 biopsy-proven IgAN patients with normal eGFR (103–141 ml/min/1.73 m^2; group IgAN-2; mean age 29.4). The urine of the 25 IgAN-1 and 25 IgAN-2 patients was a first-morning sample collected at baseline as part of the NEFIGAN clinical trial [20] ahead of randomization to drug or placebo. None were receiving immunosuppressive treatment at the time of urine collection and all were European-Caucasian IgAN patients. The IgAN-1 and IgAN-2 urine samples were compared initially with 15 healthy European-Caucasian volunteers with no known kidney disease (mean age 33.5). These samples were used as healthy controls for urine ELISA measurements as indicated. From the 25 IgAN-1 and 25 IgAN-2 NEFIGAN clinical trial [20] patients, we also used their matching serum samples for ELISA measurements as indicated in Results. Serum samples were also collected before pharmacological interventions. The NEFIGAN serum samples were compared (ELISA) with 25 sex and age matched serum samples collected from healthy subjects without renal disease at the John Walls Renal Unit. All urine and serum samples were spun to remove cells and debris before freezing. Urine and serum samples were frozen is smaller aliquots to minimize freeze-thaw cycles. Urine and serum samples were slowly defrosted on ice before experimental procedures. All tissue and biofluid samples were collected, processed and archived at the John Walls Renal Unit and kept at -80 °C. Finally, we isolated peripheral blood mononuclear cells (PBMCs) from 7 healthy donors using standard Histopaque-1077 (Merck) procedure. PBMCs were taken from the buffy coat while granulocytes were obtained from Histopaque pellets by lysing red blood cells with erythrocyte lysis buffer (Roche) twice for 5 min. All cells were cultured in RPMI plus 10% foetal calf serum. Normal adult human mesangial cells and DAKIKI cell line (human IgA^+ B-cell lymphoma [21]) were obtained from ATCC.

3. Results

Shotgun LC-MS/MS (Q-Exactive) proteomics analysis on 500 μl of albumin and IgG-depleted urine identified 325 proteins with high mass-accuracy (10 ppm) and at least 2 unique peptides (Supplemental Tables 1 and 2). Albumin and IgG depletion of urine was utilised before proteomics to reduce the concentration of the 2 most abundant protein species in IgAN urine and thereby improve the dynamic range of protein identifications. All identified proteins and spectral counts are provided in Supplemental Table 1. Full dataset peptide and protein details are provided in Supplemental Table 2. Raw MS files have been deposited and made freely accessible in *Mendeley Data* (https://bit.ly/30Baxpc) to facilitate open data access. Proteomics measured an increase in multiple immunoglobulins (including IgA) in IgAN urine together with an increase in complement C3 (Supplemental Table 1). The classic marker of renal damage, cystatin-C (CSTC), was increased in IgAN urine while uromodulin (UMOD) a biomarker of normal renal function, was decreased as expected (Supplemental Table 1). Notably, we were not able to completely remove albumin and IgG from urine samples used for proteomics (Supplemental Table 1), likely due to overwhelming proteinuria affecting IgAN patients.

We then submitted the 325 identified urine proteins to full gene ontology (GO) analysis [22] which includes "*Biological process*", "*Molecular function*" and "*Cellular component*" GO categories, to isolate the main protein classifications in our identified urine proteome (Supplemental Fig. 1). Proteins classified by GO as "*Extracellular*", dominated both healthy and IgAN urine (Supplemental Fig. 1E-F). Inflammation and proteolysis-related proteins accumulated in IgAN urine while healthy urine was enriched in adhesion and receptor-binding factors (Supplemental Fig. 1E-F). Amongst multiple proteins that have not been reported in IgAN previously (Supplemental Table 1), we noted 19 lysosomal proteins in urine (Fig. 1A) including cathepsins (CTSB, CTSC, CTSD, CTSZ), proteolytic inhibitors (cystatins; CSTA, CSTB, CST3, CST6) as well as other less studied proteins (ACPP, ARSA, NCP2, PEBP4). The presence of lysosomal proteins might be the result of exosome secretion in urine as previously noted [23].

Our attention was captured by PEBP4 (Fig. 1A and Supplemental Table 1) a likely lysosomal protein [14] with unknown renal function. This relatively understudied protein is possibly secreted [24] and might act as a cell survival factor in different tumours, most notably (given the involvement of B-cells in IgAN) B-cell lymphoma [15,25–27]. Elevation of PEBP4 in IgAN urine was validated first by dot-blot (Fig. 1B-C) in archived healthy and IgAN urines (from the Leicester renal bioarchive) followed by ELISA (Fig. 1D). Urine ELISA-estimated concentrations were corrected to urine creatinine (values shown in Supplemental Fig. 2A) as per standard experimental practice [19]. For comparison, we examined cathepsin Z (CTSZ; Fig. 1E), a classic lysosomal protein with unknown function in IgAN that we also detected in urine by proteomics, albeit with few spectra (Supplemental Table 1). CTSZ was

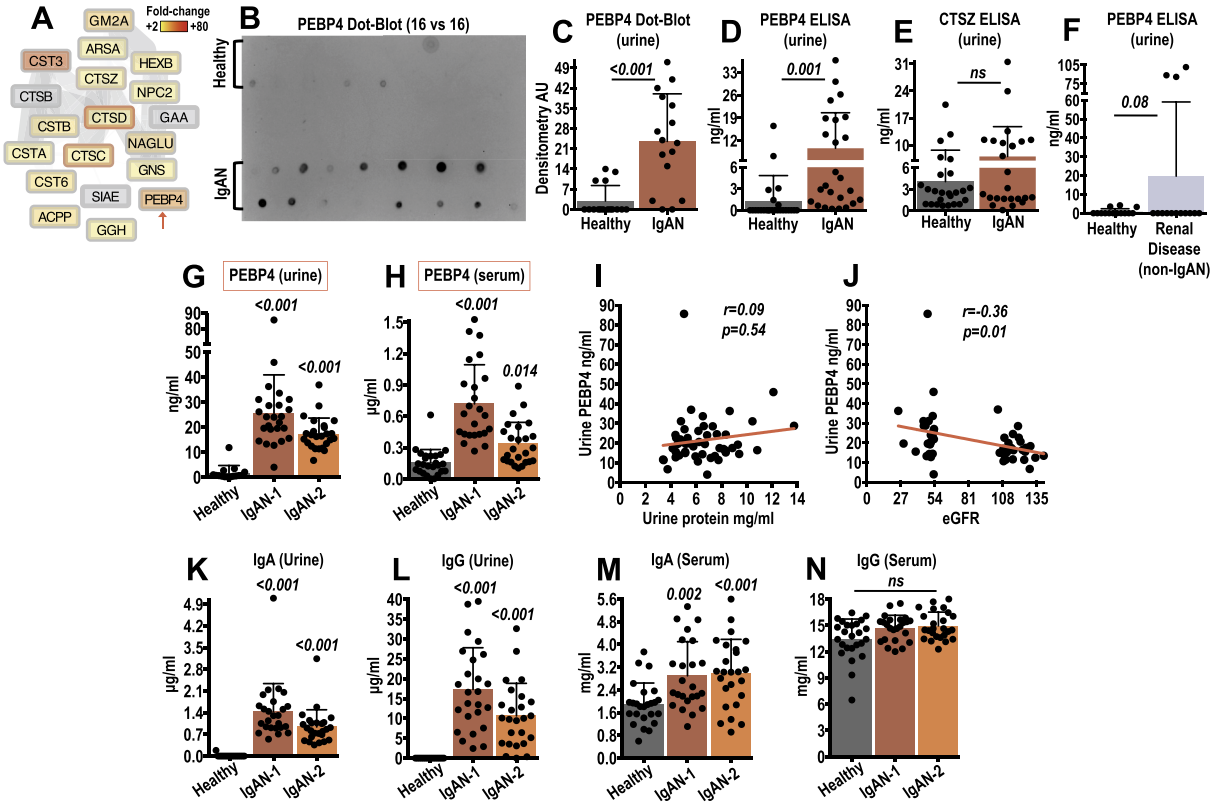

Fig. 1. PEBP4 was identified by proteomics in urine and is increased in IgAN urine and serum. **A**: LC-MS/MS Proteomics analysis of healthy donor and IgAN patient urine identified 19 lysosomal proteins including PEBP4. Lysosomal proteins were isolated from identified urine proteins using gene ontology and are presented as a colour-coded protein-protein interaction network (yellow and red are upregulated in IgAN urine as indicated, while grey are unchanged between healthy and IgAN urine. Also see Supplemental Fig. 1 and Supplemental Table 1. **B–C**: PEBP4 levels were compared in healthy and IgAN urines using dot-blot on a nitrocellulose membrane and antibodies against PEBP4 (**B**) and quantified by densitometry (**C**). 1 µl of urine was used per dot. **D-E**: PEBP4 (**D**) and CTSZ (**E**) levels were compared in a cohort of healthy or IgAN urines using ELISA. ELISA values were corrected to urine creatinine concentration measured on the same urine samples. Correcting ELISA measurements to urine creatinine is standard practice to account for differences in urine concentration and hydration. Statistical comparisons were performed using *t*-test. *t*-test *p*-values are shown on graphs; *ns*: not significant. **F**: Urine PEBP4 estimation by ELISA (creatinine-corrected) in healthy donors versus patients with non-IgAN renal disease. The 3 urine samples with high PEBP4 were from a patient with type-2 diabetes, one with chronic obstructive nephropathy and one with focal segmental glomerulosclerosis. *t*-test *p*-value shown. **G-H**: PEBP4 levels measured in healthy donor or IgAN patient urine (**G**) and serum (**H**). PEBP4 urine levels were corrected to urine creatinine as above. Two groups of IgAN urine and serum were used (IgAN-1 n = 25 and IgAN-2 n = 25) from biopsy-diagnosed IgAN patients registered in the NEFIGAN clinical trial. Patients in the IgAN-1 group had low eGFR (25–53 ml/min/1.73 m^2) while IgAN-2 group had normal eGFR (103–141 ml/min/1.73 m^2). eGFR < 60 indicates decline in renal function. Statistical estimations were performed using ANOVA and Fisher LSD post-hoc test comparing healthy subjects versus either IgAN-1 or IgAN-2 patients. Fisher LSD *p*-values are shown. **I**: No significant correlation between PEBP4 urine levels and urine protein concentration (all values are creatinine-corrected). **J**: Negative and significant correlation of patient PEBP4 urine levels (creatinine-corrected) with patient eGFR (eGFR from NEFIGAN IgAN-1 and IgAN-2 patients; see Supplemental Fig. 2C). Statistical *p* and *r* values were calculated with Pearson correlation. **K–N**: IgA and IgG levels were measured in the healthy donor or IgAN (IgAN-1 and IgAN-2 cohorts) urine and serum as indicated. Urine values are creatinine-corrected. Statistical estimations were performed using ANOVA and Fisher LSD test comparing healthy subjects versus either IgAN-1 or IgAN-2 patients. Fisher LSD *p*-values are shown. (For interpretation of the references to color in this figure legend, the reader is referred to the Web version of this article.)

not significantly altered in the same urine samples (Fig. 1E) indicating that increased urinary PEBP4 is likely not due to random release of tissue proteins in IgAN urine as a result of proteinuria. To determine the specificity of urinary PEBP4 excretion in IgAN we measured PEBP4 in the urine of 14 non-IgAN chronic kidney disease urine samples. PEBP4 was undetectable in 11 of 14 samples but highly elevated in 3 samples (Fig. 1F; “type-2 diabetes”, “chronic obstructive nephropathy” and “focal segmental glomerulosclerosis”) indicating that urinary PEBP4 excretion might not be exclusive to IgAN but is perhaps related to kidney damage or inflammation. The expression of PEBP4 in other renal diseases needs further investigation in larger patient cohorts.

To further examine urinary excretion of PEBP4, we validated its increase in a separate cohort of 50 IgAN urine samples collected at the beginning of the NEFIGAN clinical trial [20] and before pharmacological intervention (Fig. 1G). ELISA-estimated PEBP4 concentrations were creatinine-corrected and creatinine values for these samples are shown in Supplemental Fig. 2B. To determine whether there was any relationship between renal function and PEBP4 in urine, IgAN samples from the NEFIGAN cohort were split according to baseline patient estimated glomerular filtration rate of creatinine (eGFR; shown in Supplemental Fig. 2C). eGFR is used as a measure of renal filtration and values < 60 ml/min/1.73 m^2 point towards impaired kidney function. 25 IgAN patients had low eGFR (25–53 ml/min/1.73 m^2; IgAN-1 group Fig. 1G) while 25 IgAN patients had normal range eGFR (103–141 ml/min/1.73 m^2; IgAN-2 Fig. 1G). ELISA validated the significant increase of PEBP4 in IgAN urine and notably, PEBP4 was significantly higher in patients with low eGFR (IgAN-1 Fig. 1G). In total 49 out of 50 IgAN-1 and IgAN-2 patients had detectable PEBP4 in their urine (4–85 ng/ml). PEBP4 was also detected in healthy and IgAN human serum and comparatively at higher concentrations than in urine (Fig.1H; 102-1,526 ng/ml). Again, PEBP4 was significantly increased in IgAN serum with a clear elevation in IgAN-1 patients (Fig. 1H). Finally while there was no significant correlation between PEBP4 and protein concentration in IgAN urine (Fig. 1I), indicating that PEBP4 is likely not related to non-selective proteinuria, there was a significant negative correlation between PEBP4 and eGFR in IgAN patients (Fig.1J; $r = -0.35$, $p = 0.01$)

suggesting that urinary PEBP4 is increased with more kidney damage. Thus, PEBP4 is a soluble protein present in serum and urine, is upregulated in IgAN and its elevation correlates with reduced kidney function.

Similar to PEBP4, IgA and IgG were elevated in IgAN urine and were higher in IgAN-1 patients (Fig. 1K-L). IgA was also increased in the serum of IgAN patients (Fig. 1M; no difference between IgAN-1 and IgAN-2 cohorts), while serum IgG was consistent across healthy and IgAN donors (Fig. 1N). Many previous studies have shown elevated circulating and urine IgA (and IgA1 immune-complexes) in IgAN patients [3,4,28]. There was a greater number of male IgAN patients in the NEFIGAN cohort (36 males vs 14 females), but no gender-specific difference in urinary PEBP4 (Supplemental Fig. 2D). In contrast, IgAN-1 patients (low eGFR) had significantly higher mean age (43.2 years) in comparison to IgAN-2 patients (normal eGFR) and 29.4 years (Supplemental Fig. 2E). This might explain differences in renal function and as a result differences in urine PEBP4. Finally, while asymptomatic urinary tract infections cannot be categorically excluded, we found no difference in urine endotoxin in healthy or IgAN patients (Supplemental Fig. 2F). Urinary tract infections might alter the immune response and as a result affect protein composition in urine (especially immunoglobulins).

Next, we set out to determine whether PEBP4 was expressed in the kidney. IgAN and healthy (transplant donors with no renal disease) kidney biopsies from the Leicester renal archive were immunostained with PEBP4 together with different proteins (Fig. 2). First, PEBP4 co-localised with a proportion of IgA immunostaining (Fig. 2A; PEBP4 red, IgA green) in IgAN glomeruli and in the lumen of renal tubules (Fig. 2A). Luminal staining perhaps explains the release of PEBP4 in urine. While this strong and sporadic PEBP4 immunoreactivity was not found in healthy biopsies (Fig. 2B), weak PEBP4 staining was seen in IgAN and healthy renal tubules (Fig. 2A-B) consistent with reported ubiquitous staining of PEBP4 in human tissues (www.proteinatlas.org). Second, in IgAN PEBP4 was in close proximity with vimentin$^+$ cells in glomeruli (Fig. 2C; predominantly mesangial and endothelial cells) but the two proteins did not colocalise (Fig. 2C). Fig. 2D depicts healthy biopsies. Third, PEBP4 did not colocalise with CD64$^+$ phagocytes (Fig. 2E; CD64 green; CD64 will primarily stain macrophages and neutrophils) decorating glomeruli and inflammatory IgAN lesions in the kidney interstitium (Fig. 2E). Fig. 2F depicts healthy biopsies.

Closer examination of high-magnification IgAN images (Fig. 2G; IgA-PEBP4 and Fig. 2H; PEBP4-vimentin) revealed that PEBP4 was localised in structures that resemble blood vessels immediately adjacent to glomeruli and thus most likely glomerular arterioles (Fig. 2G-H; the endothelial layer of the vessel in Fig. 2H is stained green with vimentin). Notably, identification of PEBP4 within blood vessels was very rare, perhaps because of the dynamic nature of blood circulation as well as tissue embedding and cutting conditions that are outside our technical control. These examples indicate that PEBP4 is likely infiltrating from the circulation. The upregulation of PEBP4 in IgAN serum (Fig. 1H) further supports the conclusion that PEBP4 might enter the kidney from the peripheral circulation.

The relationship of PEBP4 with IgA, the key pathogenic factor in IgAN and a marker of B-cells [29,30], was surprising. To investigate this further we stained tissue biopsies for CD19, a classic marker of B-cells (Fig. 3A). PEBP4 colocalised with CD19 and IgA in IgAN glomeruli and in the lumen of tubules (Fig. 3A). Areas with IgA staining alone (without CD19 or PEBP4 immunoreactivity) represent mesangial IgA deposition as per typical IgAN histopathology. Thus, strong PEBP4 immunopositivity is likely related to infiltrating CD19$^+$/IgA$^+$ B-cells.

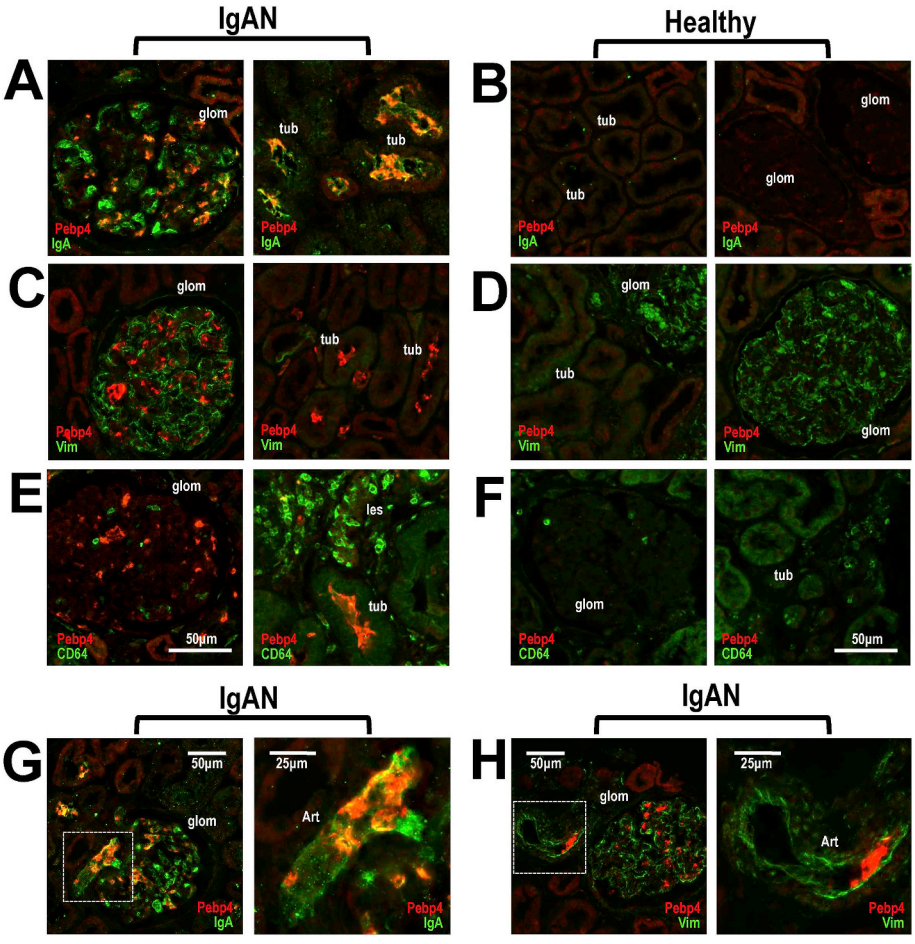

Fig. 2. PEBP4 immunofluorescence in renal biopsy specimens. **A-B**: Sporadic clusters of strong PEBP4 immunoreactivity (red) were observed in IgAN glomeruli (**A**; *glom*) and in the lumen of IgAN tubules (**A**; *tub*). In IgAN specimens (**A**) PEBP4 (red) and IgA (green) colocalise in glomeruli (*glom*) and in the lumen of tubules (*tub*). Note that not all IgA immunoreactivity is associated with PEBP4. In healthy biopsies (**B**), there was only weak PEBP4 immunoreactivity in renal tubules (also seen in IgAN), but no evidence of the strong, sporadic PEBP4 immunostaining seen in IgAN specimens. **C-D**: PEBP4 (red) in IgAN glomeruli (**C**) does not colocalise with vimentin (green). PEBP4 is strongly immunoreactive in the lumen of IgAN renal tubules (**C**). Healthy kidneys (**D**) have vimentin staining in glomeruli (**D**) but there is little PEBP4 immunostaining. Vimentin stains mainly mesangial and endothelial cells. ***E-F***: PEBP4 (red) does not colocalise with CD64$^+$ phagocytes (green) in IgAN biopsies (**E**). Few CD64$^+$ cells can be seen in IgAN glomeruli (**E**) but many accumulate in interstitial lesions (**E;** *les*). Weak CD64 staining (few isolated cells) can be seen in healthy kidney biopsies (**F**). **G-H**: In two IgAN specimens stained with either IgA (**G**) or Vimentin (**H**) we noted strong PEBP4 immunostaining within structures that resemble glomerular arterioles (*Art*), next to glomeruli. These structures are depicted in white dashed boxes and magnified as shown. (For interpretation of the references to color in this figure legend, the reader is referred to the Web version of this article.)

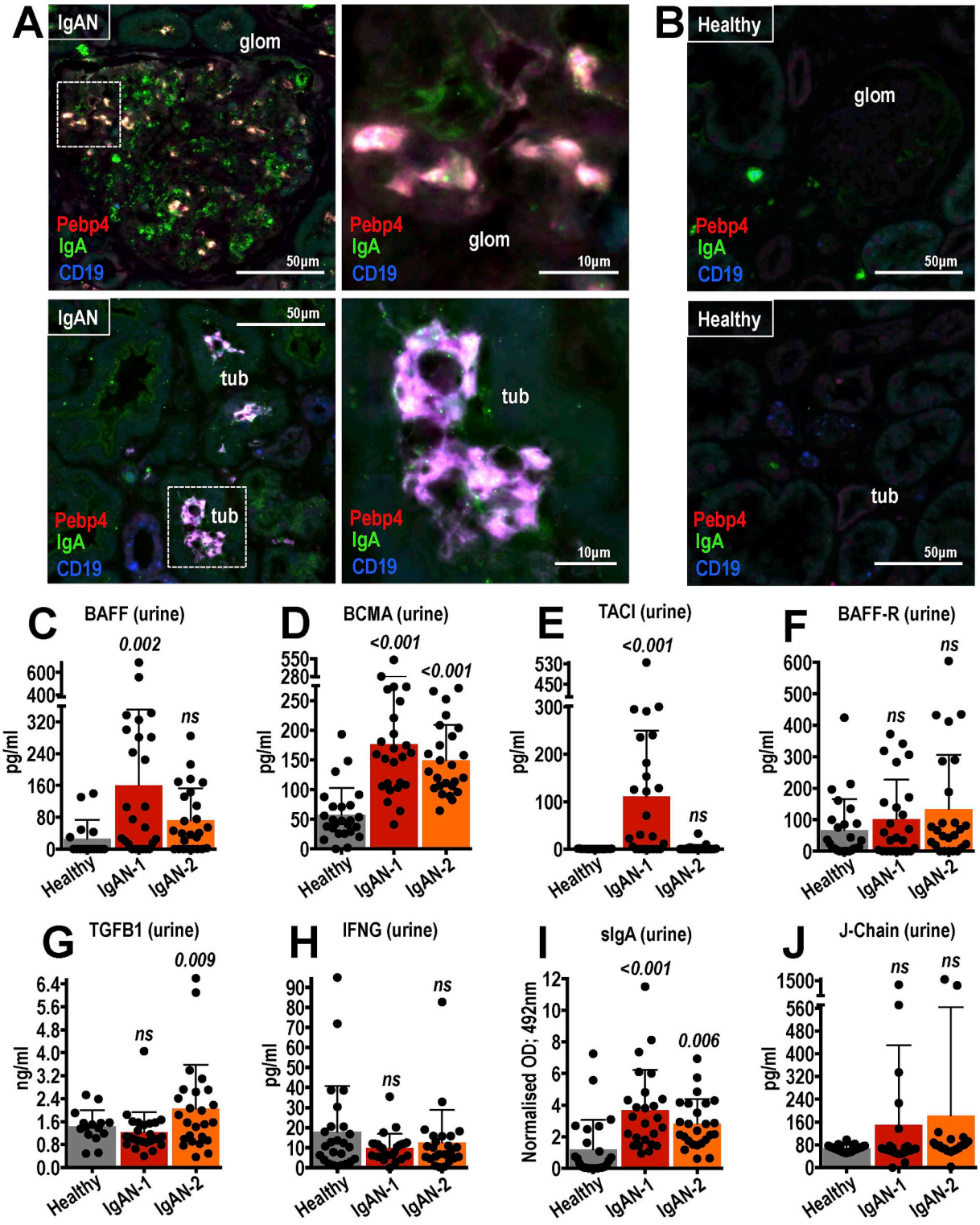

Fig. 3. Association of PEBP4 with CD19 and IgA in IgAN lesions and B-cell related proteins in urine. **A**: In few IgAN specimens PEBP4 (red), colocalised with the B-cell marker CD19 (blue) and IgA (green) in glomeruli and in the lumen of IgAN tubules. White dashed boxes (**A**) depict areas that are magnified in adjacent images. Note that not all IgA + areas in IgAN glomeruli (**A**) are PEBP4 + /CD19 + . Single IgA immunostaining likely depicts typical mesangial IgA deposits in IgAN. **B**: Healthy donor biopsies have weak immunostaining as before. **C-J**: Levels of different soluble factors involved in B-cell activation and IgA class-switch are estimated by ELISA in healthy and IgAN urine. BAFF (**C**) and its receptors BCMA (**D**) and TACI (**E**) were increased in IgAN urine, especially in IgAN-1 patients (low eGFR, reduced renal function group). BAFF-R (**F**) was unchanged in urine. Urinary TGFB1 (**G**) is significantly different between healthy and IgAN-2 subjects but not between healthy and IgAN-1. IFNG (**H**) was unchanged. Secretory IgA (sIgA; **I**) was increased in IgAN urine while J-chain (**J**) was unchanged. All values are creatinine corrected as before. Statistical analysis was performed using ANOVA and Fisher LSD post-hoc comparisons, testing IgAN-1 and IgAN-2 groups versus healthy subjects; post-hoc *p*-values are indicated on graphs. *ns*; not significant. Please note that for in-house made sIgA ELISA (**I**), differences were estimated by normalised OD rather than absolute concentrations [17]. (For interpretation of the references to color in this figure legend, the reader is referred to the Web version of this article.)

Nevertheless, it is important to note that while PEBP4 was increased (ELISA) in the overwhelming majority of IgAN urines and sera tested, as well as in few healthy samples (Fig. 1B-D and Fig. 1G-H), we were only able to find strong PEBP4 immunoreactivity and costaining with CD19 and IgA in just 3 out of 8 IgAN biopsies. In the remaining biopsies and in healthy controls (Figs. 3B and 2B, D, F), PEBP4 was weakly expressed in renal tubules, in agreement with (antibody-based) expression of PEBP4 in most tissues (Human Protein Atlas; www.proteinatlas.org). The presence of circulating $CD19^+$ B-cells infiltrating IgAN kidneys has been previously documented in 3 studies [8,31,32] but surprisingly their exact immunophenotype or function in IgAN kidney has not been examined in detail thus far, perhaps because they are few and hard to identify in the tissue. IgAN kidney biopsies are also very small making such efforts challenging.

Another disease with substantial B-cell involvement is systemic lupus erythrematosus (SLE). The most common pathological manifestation of SLE patients is nephritis (lupus nephritis), characterised by renal accumulation of immune complexes (including IgA) and B-cell infiltration [33,34]. To this end, we found PEBP4-IgA costaining on kidney biopsies from 2 SLE patients with nephritis (Supplemental Fig. 3). Most of the sporadic PEBP4-IgA colocalisation was seen in affected glomeruli and in the interstitium between renal tubules, but unlike IgAN specimens, not in the lumen of tubules.

The association of PEBP4 with IgA and CD19 prompted us to examine more B-cell related proteins in IgAN urine, especially those involved in IgA class-switch and expression (Fig. 3C-J). Like PEBP4, B-cell activating factor (BAFF) [12] was significantly increased in the urine of IgAN-1 patients (low eGFR) but not IgAN-2 patients (normal eGFR) (Fig. 3C). In contrast to PEBP4, BAFF was unchanged in serum (Supplemental Fig. 2G) indicating the complexity in soluble factor regulation in biofluids and the likely importance of urine as a more selective pool for bioactive factors. The B-cell-specific BAFF/APRIL receptor BCMA [35] (B-cell maturation antigen or TNFRSF17) together with TACI (transmembrane activator and CAML interactor or TNFRSF13B) another BAFF/APRIL receptor expressed on B- and T-cells [36], were increased in IgAN urine and further elevated in IgAN-1 (low eGFR) patients (Fig. 3D-E). TACI was very low in IgAN-2 samples. In contrast to BCMA and TACI, the third specific BAFF receptor, BAFF-R (or TNFRSF13C), was unchanged between healthy and IgAN donors (Fig. 3F). We also examined two T-cell derived cytokines TGFβ1 and IFNγ, also involved in immunoglobulin regulation by B-cells. TGFβ1 (IgA class-switch) was present in healthy and IgAN urine and was modestly increased in IgAN-2 patients (Fig. 3G), while low levels of IFNγ (IgG2 expression) were detected in urine but the cytokine was unchanged between healthy and IgAN samples (Fig. 3H). Finally, while secretory IgA (sIgA) was increased in both IgAN-1 and IgAN-2 urine (Fig.3I), J-chain link protein (necessary for sIgA mucosal secretion) was unchanged (Fig. 3J). This might be due to the fact that J-chain incorporated in sIgA is masked by the associated IgA molecules (as it is not in free form) and perhaps explains why it is not consistently detected by ELISA in urine. Increased sIgA in the serum and urine of IgAN patients has been routinely reported and is likely related to IgAN pathophysiology [37,38]. The presence of sIgA in normal urine is also expected (and in high concentrations) given its presence in the urinary mucosa.

In summary, alongside PEBP4, classic factors associated with IgA class-switch and IgA expression on B-cells are elevated in IgAN urine. It is important to note however that apart from the proteins mentioned above, we also tested the urine for other B-cell relevant proteins, including CD19, APRIL, IL6, IL10 and CD138 (marker of plasma B-cells) but all were undetectable in either healthy or IgAN urine. Similarly, urine proteomics analysis did not detect specific B-cell factors or B-cell "CD" markers but this might be related to the limit of LC-MS/MS detection (such cellular markers are not likely to be soluble and abundant in biofluids) and the fact that urine samples were spun to remove cellular debris before processing.

The possible immune-related or kidney function of PEBP4 is unknown. The Human Protein Atlas reports ubiquitous staining of PEBP4 in most normal human organs and highest expression in tonsil and spleen, tissues high in B-cells. Similarly, sequence of different cell lines (and published work - [27]) suggests highest PEBP4 expression in myeloma B-lymphocytes (NCBI BioProject PRJNA183192; www.proteinatlas.org). To obtain an unbiased overview on possible molecular functions of PEBP4, we examined its expression in published microarray datasets derived from the European Bioinformatics Institute (EBI) ArrayExpress public repository. While PEBP4 was differentially regulated in multiple cancer-related studies, we found that it was upregulated in a more relevant microarray dataset derived from the classic monocytic cell line THP1 stimulated with 100 ng/ml IFNγ for 3 days. (ArrayExpress EBI; *E*-MTAB-5917). Notably, PEBP4 was weakly upregulated in THP1 cells only following stimulation with IFNγ and not after LPS or combined LPS-IFNγ stimulation. 1937 genes were upregulated alongside PEBP4 following IFNγ stimulation (Supplemental Fig. 4; differential expression data was downloaded from *E*-MTAB-5917). We then used protein-protein interaction network analysis to find first-degree neighbours of PEBP4, i.e. IFNγ-induced genes in THP1 cells directly interacting with PEBP4 (Fig. 4A). The PEBP4 interactome (Fig. 4A) contains 41 inflammation-related genes including the TNF-family cytokine TRAIL (TNFSF10), B-cell proteins KMO and ADAM28, as well as MAPK1 (ERK2 MAP-kinase) and the TGF-family growth factor BMP1 (Fig. 4A). Similar to urine proteomics, the 2 top GO functional enrichments for this gene cluster include "*Extracellular region*" (Fig. 4B) and "*Lysosome*" (Fig. 4C). Lysosomal proteins cathepsin-B (CTSB) and aryl sulfatase-A (ARSA), were also found in IgAN urine (Fig. 1A and Supplemental Table 1).

In cell culture experiments, an IgA^+ monoclonal B-cell line (DAKIKI human B-cell lymphoma [21]) expressed higher levels of PEBP4 in comparison to human mesangial cells (Fig. 4D). PEBP4 protein was also more abundant in peripheral PBMCs in contrast to granulocytes from the same donors (Fig. 4E). When cultured human PBMCs were stimulated for 24 h with different cytokines (Fig. 4F-G), IFNγ caused a clear increase in the secretion of PEBP4 in the PBMC culture medium from 7 healthy donors (Fig. 4G) but without causing notable alteration in PEBP4 expression in the same PBMC cellular lysates (Fig. 4F; representative blot). Thus, PEBP4 is likely a secreted protein and its secretion by human PBMCs *in vitro* is enhanced by IFNγ. It is important to highlight that urinary IFNγ was not increased in IgAN patients (Fig. 3H) and thus we cannot speculate whether there is a functional link between IFNγ and increased soluble PEBP4 in IgAN *in vivo*.

4. Discussion

PEBP4 is a ubiquitous and evolutionary conserved but scarcely studied protein that like the other PEBP family members (PEBP1-4), potentially binds phosphatidylethanolamine and might act as a serine protease inhibitor [14]. 15 years ago, mechanistic experiments that have not received further attention, indicated that PEBP4 is mainly lysosomal and responds to TNFα treatment by translocating to the cell membrane where it binds with ERK kinase MEK1 and inhibits TNFα induced activation of ERK via RAF1 and MEK1 [14,15]. More recent work has shown over-expression of PEBP4 in multiple tumours and a likely anti-apoptotic function that promotes cancer development and metastasis [15,25–27]. The protein might also participate in epithelial-to-mesenchymal transition (EMT) in small cell lung cancer by activating the sonic hedgehog pathway [25].

The possible IgAN function of PEBP4 is unknown. We found that PEBP4 was consistently upregulated in IgAN urine and serum. The possibility that this protein might be a disease biomarker needs to be examined further and prospectively to understand if it is linked to the risk of IgAN progression. The possible sensitivity of PEBP4 is also unknown but it needs to be examined further given that PEBP4 is also found in few healthy serum and urine samples. Future studies in larger

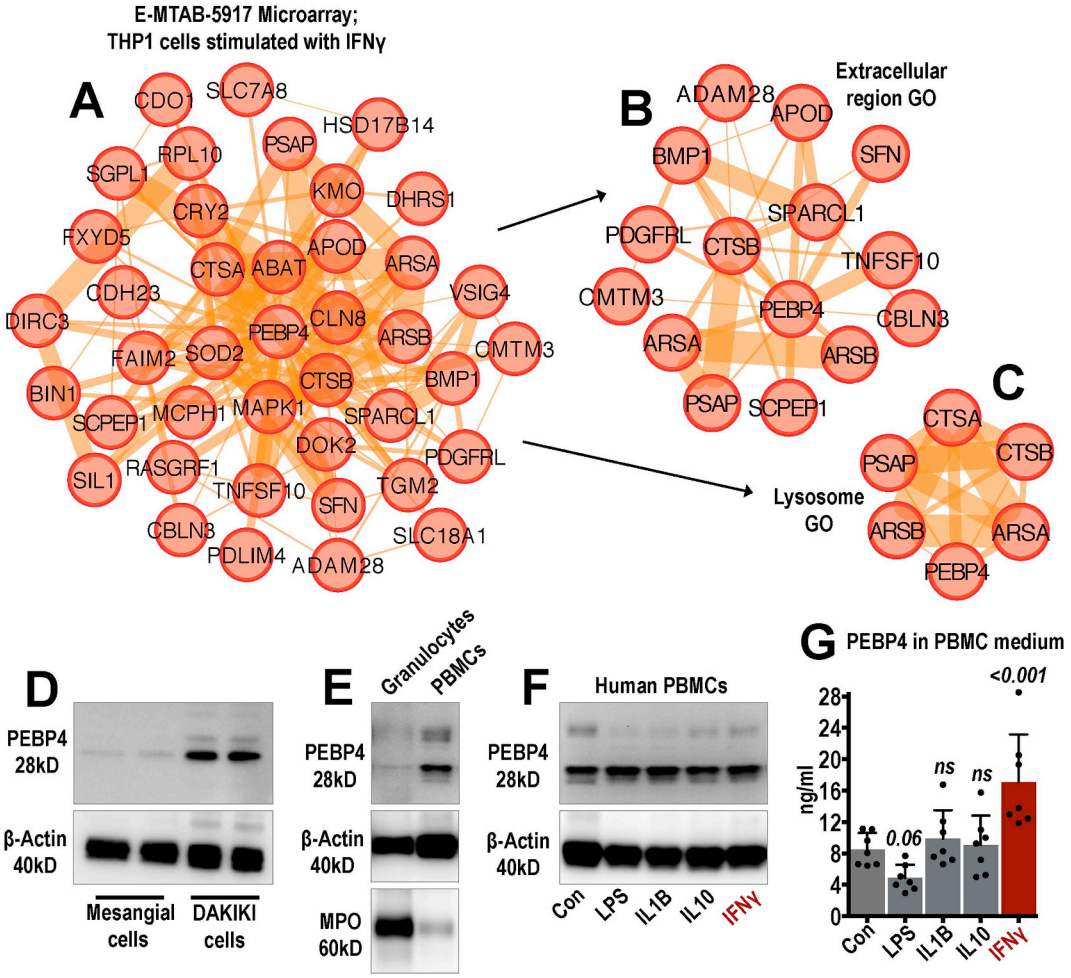

Fig. 4. Investigating PEBP4 expression in cells. A-C: 41 PEBP4 first neighbour genes (PEBP4 interactome; **A**) were isolated from the protein-protein interaction network of upregulated genes derived from a published microarray analysis of THP1 cells stimulated with IFNγ (100 ng/ml) for 3 days (*E*-MTAB-5917; ArrayExpress EBI; see Supplemental Fig. 4). The PEBP4 interactome (**A**) is enriched in "*Extracellular region*" and "*Lysosome*" gene ontology (GO) categories and relevant genes are isolated in (**B**) and (**C**) respectively. Protein-protein interaction networks were created using data from StringDB and designed in Cytoscape. Gene Ontology (GO) was analysed using BinGO in Cytoscape. **D**: PEBP4 expression in human primary mesangial cells and DAKIKI cells (human IgA$^+$ B-cell lymphoma) was examined in cell lysates by immunoblotting. Cells were cultured for 3 days before lysis in 0.2% SDS. 20 μg of cellular protein was immunoblotted. β-Actin served as the loading control. **E**: Granulocytes and PBMCs were isolated from human EDTA-treated blood using standard protocol. Cells were cultured for 24 h before lysis. 20 μg of cellular protein was immunoblotted. PBMC lysates contain more PEBP4 while granulocyte lysates are enriched in myeloperoxidase (MPO; neutrophil marker). A representative blot is shown. **F-G**: PBMCs were isolated, cultured and stimulated for 24 h with either 1 μg/ml LPS or 150 ng/ml IL1β, IL10 and IFNγ. Control PBMCs were unstimulated (Con). PBMC lysates were immunoblotted for PEBP4 (**F**) while the PBMC culture medium was used to detect PEBP4 by ELISA (**G**). Statistical analysis was performed using ANOVA and Fisher LSD post-hoc comparisons, testing the effect of different cytokines versus unstimulated cells (Con); post-hoc *p*-values are indicated on graphs. *ns*; not significant. IFNγ caused a clear increase in the release of PEBP4 in the PBMC culture medium 24 h after stimulation (**G**) while LPS reduced PEBP4 (close to significant). Note that there was no observable change in PEBP4 levels in PBMC lysates (**F**).

patient cohorts combining IgAN and other renal diseases are necessary given that PEBP4 was increased in the urine of 3 non-IgAN patients as well as in 2 lupus nephritis biopsies, the latter characterised by B-cell infiltration in the kidney [33,34]. Elevated PEBP4 might not be exclusive to IgAN but it might be a marker of renal damage or perhaps a by-product of immune activation that involves B-cells.

PEBP4 sporadically colocalised with IgA and CD19 in few IgAN biopsies indicating that it might be related to circulating IgA$^+$ B-cells [29,30] infiltrating IgAN lesions. The origin of PEBP4 from the circulation was further supported by its localisation within glomerular arterioles and its upregulation in IgAN serum. In addition, the increase in urinary PEBP4 coincided with an increase in IgA class-switch molecules BAFF, BCMA, TACI and TGFβ1 in IgAN urine, indicating B-cell activation towards IgA expression in IgAN patients.

Nevertheless, linking PEBP4 with B-cell activity and function in IgAN tissue and urine was not conclusive. For instance, in contrast to BAFF, BCMA and TACI, BAFF-R (which is BAFF-specific) was unchanged between healthy and IgAN subjects, while we failed to detect by ELISA other key B-cell proteins in urine, including CD19 and IgA class-switch cytokines APRIL, IL6 and IL10. It is possible that PEBP4 is linked to a specific B-cell response taking place in IgAN and involving only specific factors (i.e. BAFF, BCMA, TACI), but it is also possible that some cytokines and B-cell proteins are not abundant and therefore difficult to detect. Thus, we provide evidence that PEBP4 is associated with IgA$^+$/CD19$^+$ cells as well as B-cell factors in urine, but more work is needed in future studies to characterise the exact phenotype of PEBP4$^+$ cells in IgAN and perhaps in other renal pathologies.

Moreover, although B-cells have been extensively studied in relation to IgAN in blood and peripheral tissues [8,39,40], infiltration of circulating B-cells in IgAN kidneys has been reported in just 3 studies [8,31,32]. Their possible regulation and immunological function in the kidney is incompletely understood, but they might target autoreactive immune-complexes [8]. IgA class-switch factors and related mechanisms in IgAN are also gaining specific attention [41–43] mainly as

regulators of IgA overexpression by B-cells [44] and as possible therapeutic targets, with a particular focus on BAFF and APRIL [36]. Exact multi-marker phenotyping and bioactivity profiling of circulating, mucosal or kidney infiltrating B-cells in IgAN has not been performed thus far using high-throughput transcriptomics or proteomics approaches but it is an important area for future research and clinical work. Such efforts might inform therapies targeting the bioactivity of B-cells in IgAN. Recent studies are moving towards this direction [8].

The possible function of PEBP4 on B- or other immune cells is also unknown and due to lack of knowledge about this protein it is challenging to speculate. Given the function of PEBP-family proteins in binding phosphatidylethanolamine [14], PEBP4 might bind secreted IgA coming in contact with the cellular membrane and this could explain the colocalisation of IgA and PEBP4 in tubules and their soluble coexpression in serum and urine. Given its anti-apoptotic role in B-cell lymphoma [27], PEBP4 might be involved in the survival and/or maintenance of B-cells in IgAN. Interestingly, by searching high-throughput gene expression data in published microarray datasets, we found that PEBP4 was upregulated in monocytic THP1 cells following stimulation with IFNγ. More importantly, IFNγ stimulation caused a consistent secretion of PEBP4 from cultured human PBMCs. Thus, PEBP4 is a secreted soluble protein - an essential property for a biomarker candidate or bioactive factor - and responds to IFNγ stimulation. The possible soluble/secreted function of PEBP4 needs to be studied in future mechanistic studies to understand whether it is bioactive in IgAN and if bioactivity is linked to IFNγ inflammatory regulation. The role of IFNγ in IgAN has been examined since the 1990's but not much is known other than the fact that the cytokine is increased in IgAN PBMCs [45], including B-cells [32], and that it accumulates in IgAN lesions [46,47]. The function of IFNγ in IgAN is an interesting area for further work, especially because the cytokine stimulates the production of IgG2 by B-cells [48,49].

PEBP4 was identified here fortuitously while we were developing methodology to analyse small quantities of IgAN urine by proteomics. Modern high-throughput proteomics can play an important role in the discovery of pathological bioactive proteins and disease biomarkers. In comparison to transcriptomics, which measure rapidly fluctuating mRNA changes, proteomics can quantify proteotypic changes and protein accumulation taking place in diseased tissues and can measure cellular tissue proteins, as well as secreted and soluble tissue proteins in the extracellular environment and in biofluids [16]. Urine is an excellent reservoir for soluble bioactive proteins and likely biomarkers and it is encouraging that a number of recent studies have targeted IgAN urine using proteomics [23,50–52]. Although most studies have used large, unpractical volumes of highly concentrated urine and complicated protocols for protein processing, we believe that it is important to focus future efforts on small urine volumes coupled to ultra-high resolution mass-spectrometers in order to increase the clinical application of urine proteomics using current technology. An important implication of our work is that non-invasive urinary analysis (either by proteomics or by targeting specific protein markers) could be utilised to monitor immunological bioactivity as well as response to therapeutic strategies in IgAN and other kidney diseases.

Taken together, PEBP4 is a new soluble IgAN-related protein. Its concentration increases in serum and urine of IgAN patients in correlation to kidney damage and is likely associated with IgA^+ B-cells infiltrating the IgAN kidney. The role of B-cells in kidney damage or tissue inflammation in IgAN is incompletely understood. The likely function of PEBP4 in IgAN pathology is unknown but its upregulation in IgAN urine and serum, and its relationship with IgA and B-cells warrants further investigation. PEBP4 might be a disease marker or a soluble bioactive factor in IgAN.

Declaration of interest

Nothing to declare.

Acknowledgements

This study was generously supported by the Mayer Family IgA Nephropathy Award (ST, JB, AD).

AD received generous funding from the Rosetrees Trust, United Kingdom (grant A1384).

JT received funding from the Volkswagen Stiftung and an Imperial College London, United Kingdom, PhD studentship.

The authors would like to thank the undergraduate student Joshua Davis and postgraduate student Somia Ahmad for valuable assistance in the lab. The authors would like to thank Lead Research Nurse Justyna Szklarzewicz for organising phlebotomy for human blood collection.

Appendix A. Supplementary data

Supplementary data to this article can be found online at https://doi.org/10.1016/j.jaut.2019.102309.

References

[1] S.C. Yeo, C.K. Cheung, J. Barratt, New insights into the pathogenesis of IgA nephropathy, Pediatr. Nephrol. 33 (2018) 763–777.
[2] A.W. van den Wall Bake, M.R. Daha, J. Radl, J.J. Haaijman, A. Van der Ark, R.M. Valentijn, L.A. Van Es, The bone marrow as production site of the IgA deposited in the kidneys of patients with IgA nephropathy, Clin. Exp. Immunol. 72 (1988) 321–325.
[3] B. Knoppova, C. Reily, N. Maillard, D.V. Rizk, Z. Moldoveanu, J. Mestecky, M. Raska, M.B. Renfrow, B.A. Julian, J. Novak, The origin and activities of IgA1-containing immune complexes in IgA nephropathy, Front. Immunol. 7 (2016) 117.
[4] Z. Moldoveanu, R.J. Wyatt, J.Y. Lee, M. Tomana, B.A. Julian, J. Mestecky, W.Q. Huang, S.R. Anreddy, S. Hall, M.C. Hastings, et al., Patients with IgA nephropathy have increased serum galactose-deficient IgA1 levels, Kidney Int. 71 (2007) 1148–1154.
[5] C. Czerkinsky, W.J. Koopman, S. Jackson, J.E. Collins, S.S. Crago, R.E. Schrohenloher, B.A. Julian, J.H. Galla, J. Mestecky, Circulating immune complexes and immunoglobulin A rheumatoid factor in patients with mesangial immunoglobulin A nephropathies, J. Clin. Investig. 77 (1986) 1931–1938.
[6] P. Aucouturier, R.C. Monteiro, L.H. Noel, J.L. Preud'homme, P. Lesavre, Glomerular and serum immunoglobulin G subclasses in IgA nephropathy, Clin. Immunol. Immunopathol. 51 (1989) 338–347.
[7] H. Suzuki, K. Kiryluk, J. Novak, Z. Moldoveanu, A.B. Herr, M.B. Renfrow, R.J. Wyatt, F. Scolari, J. Mestecky, A.G. Gharavi, et al., The pathophysiology of IgA nephropathy, J. Am. Soc. Nephrol. 22 (2011) 1795–1803.
[8] C. Huang, X. Li, J. Wu, W. Zhang, S. Sun, L. Lin, X. Wang, H. Li, X. Wu, P. Zhang, et al., The landscape and diagnostic potential of T and B cell repertoire in immunoglobulin A nephropathy, J. Autoimmun. 97 (2019) 100–107.
[9] D. Schlondorff, B. Banas, The mesangial cell revisited: no cell is an island, J. Am. Soc. Nephrol. 20 (2009) 1179–1187.
[10] K. Molyneux, D. Wimbury, I. Pawluczyk, M. Muto, J. Bhachu, P.R. Mertens, J. Feehally, J. Barratt, beta1,4-galactosyltransferase 1 is a novel receptor for IgA in human mesangial cells, Kidney Int. 92 (2017) 1458–1468.
[11] J. Barratt, S.C.W. Tang, Treatment of IgA nephropathy: evolution over half a century, Semin. Nephrol. 38 (2018) 531–540.
[12] R. Coppo, Biomarkers and targeted new therapies for IgA nephropathy, Pediatr. Nephrol. 32 (2017) 725–731.
[13] R.N. Moresco, M.M. Speeckaert, J.R. Delanghe, Diagnosis and monitoring of IgA nephropathy: the role of biomarkers as an alternative to renal biopsy, Autoimmun. Rev. 14 (2015) 847–853.
[14] X. Wang, N. Li, B. Liu, H. Sun, T. Chen, H. Li, J. Qiu, L. Zhang, T. Wan, X. Cao, A novel human phosphatidylethanolamine-binding protein resists tumor necrosis factor alpha-induced apoptosis by inhibiting mitogen-activated protein kinase pathway activation and phosphatidylethanolamine externalization, J. Biol. Chem. 279 (2004) 45855–45864.
[15] R.Q. Huang, S.Q. Wang, Q.B. Zhu, S.C. Guo, D.L. Shi, F. Chen, Y.C. Fang, R. Chen, Y.C. Lu, Knockdown of PEBP4 inhibits human glioma cell growth and invasive potential via ERK1/2 signaling pathway, Mol. Carcinog. 58 (2019) 135–143.
[16] A. Didangelos, M. Puglia, M. Iberl, C. Sanchez-Bellot, B. Roschitzki, E.J. Bradbury, High-throughput proteomics reveal alarmins as amplifiers of tissue pathology and inflammation after spinal cord injury, Sci. Rep. 6 (2016) 21607.
[17] D.P. Gale, K. Molyneux, D. Wimbury, P. Higgins, A.P. Levine, B. Caplin, A. Ferlin, P. Yin, C.P. Nelson, H. Stanescu, et al., Galactosylation of IgA1 is associated with common variation in C1GALT1, J. Am. Soc. Nephrol. 28 (2017) 2158–2166.
[18] L. Layward, A.C. Allen, S.J. Harper, J. Feehally, Increased IgA and decreased IgG production by Epstein-Barr virus transformed B cells in culture in IgA nephropathy, Exp. Nephrol. 2 (1994) 24–29.
[19] D.J. Newman, M.J. Pugia, J.A. Lott, J.F. Wallace, A.M. Hiar, Urinary protein and albumin excretion corrected by creatinine and specific gravity, Clin. Chim. Acta 294 (2000) 139–155.
[20] B.C. Fellstrom, J. Barratt, H. Cook, R. Coppo, J. Feehally, J.W. de Fijter, J. Floege, G. Hetzel, A.G. Jardine, F. Locatelli, et al., Targeted-release budesonide versus

placebo in patients with IgA nephropathy (NEFIGAN): a double-blind, randomised, placebo-controlled phase 2b trial, Lancet 389 (2017) 2117–2127.
[21] I. Millet, C. Samarut, J.P. Revillard, Class-specific suppression of human B cell maturation by IgA-binding factors, Eur. J. Immunol. 18 (1988) 545–550.
[22] The gene ontology resource: 20 years and still GOing strong, Nucleic Acids Res. 47 (2018) D330–D338.
[23] P.G. Moon, J.E. Lee, S. You, T.K. Kim, J.H. Cho, I.S. Kim, T.H. Kwon, C.D. Kim, S.H. Park, D. Hwang, et al., Proteomic analysis of urinary exosomes from patients of early IgA nephropathy and thin basement membrane nephropathy, Proteomics 11 (2011) 2459–2475.
[24] H. He, D. Liu, H. Lin, S. Jiang, Y. Ying, S. Chun, H. Deng, J. Zaia, R. Wen, Z. Luo, Phosphatidylethanolamine binding protein 4 (PEBP4) is a secreted protein and has multiple functions, Biochim. Biophys. Acta 1863 (2018) 1682–1689.
[25] W. Jian, Y. Bai, X. Li, J. Kang, Y. Lei, Y. Xue, Phosphatidylethanolamine-binding protein 4 promotes the epithelial-to-mesenchymal transition in non-small cell lung cancer cells by activating the sonic hedgehog signaling pathway, J. Cell. Biochem. 120 (2018) 5386–5395.
[26] W. Sun, J. Shi, J. Wu, J. Zhang, H. Chen, Y. Li, S. Liu, Y. Wu, Z. Tian, X. Cao, et al., A modified HLA-A*0201-restricted CTL epitope from human oncoprotein (hPEBP4) induces more efficient antitumor responses, Cell. Mol. Immunol. 15 (2018) 768–781.
[27] K. Wang, Y. Jiang, W. Zheng, Z. Liu, H. Li, J. Lou, M. Gu, X. Wang, Silencing of human phosphatidylethanolamine-binding protein 4 enhances rituximab-induced death and chemosensitization in B-cell lymphoma, PLoS One 8 (2013) e56829.
[28] K. Matousovic, J. Novak, T. Yanagihara, M. Tomana, Z. Moldoveanu, R. Kulhavy, B.A. Julian, K. Konecny, J. Mestecky, IgA-containing immune complexes in the urine of IgA nephropathy patients, Nephrol. Dial. Transplant. 21 (2006) 2478–2484.
[29] C. Johansson, I. Ahlstedt, S. Furubacka, E. Johnsson, W.W. Agace, M. Quiding-Jarbrink, Differential expression of chemokine receptors on human IgA+ and IgG+ B cells, Clin. Exp. Immunol. 141 (2005) 279–287.
[30] J. Prigent, V. Lorin, A. Kok, T. Hieu, S. Bourgeau, H. Mouquet, Scarcity of auto-reactive human blood IgA(+) memory B cells, Eur. J. Immunol. 46 (2016) 2340–2351.
[31] F. Heller, M.T. Lindenmeyer, C.D. Cohen, U. Brandt, D. Draganovici, M. Fischereder, M. Kretzler, H.J. Anders, T. Sitter, I. Mosberger, et al., The contribution of B cells to renal interstitial inflammation, Am. J. Pathol. 170 (2007) 457–468.
[32] H. Yuling, X. Ruijing, J. Xiang, J. Yanping, C. Lang, L. Li, Y. Dingping, T. Xinti, L. Jingyi, T. Zhiqing, et al., CD19+CD5+ B cells in primary IgA nephropathy, J. Am. Soc. Nephrol. 19 (2008) 2130–2139.
[33] A. Chang, S.G. Henderson, D. Brandt, N. Liu, R. Guttikonda, C. Hsieh, N. Kaverina, T.O. Utset, S.M. Meehan, R.J. Quigg, et al., In situ B cell-mediated immune responses and tubulointerstitial inflammation in human lupus nephritis, J. Immunol. 186 (2011) 1849–1860.
[34] C.Y. Sun, Y. Shen, X.W. Chen, Y.C. Yan, F.X. Wu, M. Dai, T. Li, C.D. Yang, The characteristics and significance of locally infiltrating B cells in lupus nephritis and their association with local BAFF expression, Internet J. Rheumatol. (2013) 954292 2013.
[35] E. Castigli, S.A. Wilson, S. Scott, F. Dedeoglu, S. Xu, K.P. Lam, R.J. Bram, H. Jabara, R.S. Geha, TACI and BAFF-R mediate isotype switching in B cells, J. Exp. Med. 201 (2005) 35–39.
[36] E. Samy, S. Wax, B. Huard, H. Hess, P. Schneider, Targeting BAFF and APRIL in systemic lupus erythematosus and other antibody-associated diseases, Int. Rev. Immunol. 36 (2017) 3–19.
[37] Y. Tan, J.J. Zhang, G. Liu, H. Zhang, M.H. Zhao, The level of urinary secretory immunoglobulin A (sIgA) of patients with IgA nephropathy is elevated and associated with pathological phenotypes, Clin. Exp. Immunol. 156 (2009) 111–116.
[38] J.J. Zhang, L.X. Xu, G. Liu, M.H. Zhao, H.Y. Wang, The level of serum secretory IgA of patients with IgA nephropathy is elevated and associated with pathological phenotypes, Nephrol. Dial. Transplant. 23 (2008) 207–212.
[39] Y.Y. Wang, L. Zhang, P.W. Zhao, L. Ma, C. Li, H.B. Zou, Y.F. Jiang, Functional implications of regulatory B cells in human IgA nephropathy, Scand. J. Immunol. 79 (2014) 51–60.
[40] Y. Suzuki, H. Suzuki, J. Nakata, D. Sato, T. Kajiyama, T. Watanabe, Y. Tomino, Pathological role of tonsillar B cells in IgA nephropathy, Clin. Dev. Immunol. (2011) 639074 2011.
[41] A. Cerutti, The regulation of IgA class switching, Nat. Rev. Immunol. 8 (2008) 421–434.
[42] G. Xin, W. Shi, L.X. Xu, Y. Su, L.J. Yan, K.S. Li, Serum BAFF is elevated in patients with IgA nephropathy and associated with clinical and histopathological features, J. Nephrol. 26 (2012) 683–690.
[43] Y.L. Zhai, L. Zhu, S.F. Shi, L.J. Liu, J.C. Lv, H. Zhang, Increased APRIL expression induces IgA1 aberrant glycosylation in IgA nephropathy, Medicine (Baltim.) 95 (2016) e3099.
[44] L. He, X. Peng, Y. Chen, G. Liu, Z. Liu, J. Zhu, Y. Liu, H. Liu, Y. Liang, F. Liu, et al., Regulation of IgA class switch recombination in immunoglobulin a nephropathy: retinoic acid signaling and BATF, Am. J. Nephrol. 43 (2016) 179–194.
[45] K.N. Lai, J.C. Leung, P.K. Li, S.F. Lui, Cytokine production by peripheral blood mononuclear cells in IgA nephropathy, Clin. Exp. Immunol. 85 (1991) 240–245.
[46] C.S. Lim, H.J. Yoon, Y.S. Kim, C. Ahn, J.S. Han, S. Kim, J.S. Lee, H.S. Lee, D.W. Chae, Clinicopathological correlation of intrarenal cytokines and chemokines in IgA nephropathy, Nephrology 8 (2003) 21–27.
[47] H. Yokoyama, M. Takaeda, T. Wada, M. Ogi, N. Tomosugi, T. Takabatake, T. Abe, M. Yoshimura, H. Kida, K. Kobayashi, Intraglomerular expression of MHC class II and Ki-67 antigens and serum gamma-interferon levels in IgA nephropathy, Nephron 62 (1992) 169–175.
[48] J. Hasbold, J.S. Hong, M.R. Kehry, P.D. Hodgkin, Integrating signals from IFN-gamma and IL-4 by B cells: positive and negative effects on CD40 ligand-induced proliferation, survival, and division-linked isotype switching to IgG1, IgE, and IgG2a, J. Immunol. 163 (1999) 4175–4181.
[49] S.L. Peng, S.J. Szabo, L.H. Glimcher, T-bet regulates IgG class switching and pathogenic autoantibody production, Proc. Natl. Acad. Sci. U. S. A. 99 (2002) 5545–5550.
[50] M. Krochmal, K. Cisek, S. Filip, K. Markoska, C. Orange, J. Zoidakis, C. Gakiopoulou, G. Spasovski, H. Mischak, C. Delles, et al., Identification of novel molecular signatures of IgA nephropathy through an integrative -omics analysis, Sci. Rep. 7 (2017) 9091.
[51] P. Prikryl, L. Vojtova, D. Maixnerova, M. Vokurka, M. Neprasova, T. Zima, V. Tesar, Proteomic approach for identification of IgA nephropathy-related biomarkers in urine, Physiol. Res. 66 (2017) 621–632.
[52] Y.W. Choi, Y.G. Kim, M.Y. Song, J.Y. Moon, K.H. Jeong, T.W. Lee, C.G. Ihm, K.S. Park, S.H. Lee, Potential urine proteomics biomarkers for primary nephrotic syndrome, Clin. Proteonomics 14 (2017) 18.